



# CANCER DISCOVERY

## Elucidating Distinct Roles for *NF1* in Melanomagenesis

Ophélia Maertens, Bryan Johnson, Pablo Hollstein, et al.

*Cancer Discovery* 2013;3:338-349. Published OnlineFirst November 21, 2012.

**Updated version** Access the most recent version of this article at:  
doi:[10.1158/2159-8290.CD-12-0313](https://doi.org/10.1158/2159-8290.CD-12-0313)

**Supplementary Material** Access the most recent supplemental material at:  
<http://cancerdiscovery.aacrjournals.org/content/suppl/2012/11/27/2159-8290.CD-12-0313.DC1.html>

**Cited Articles** This article cites by 57 articles, 17 of which you can access for free at:  
<http://cancerdiscovery.aacrjournals.org/content/3/3/338.full.html#ref-list-1>

**Citing articles** This article has been cited by 1 HighWire-hosted articles. Access the articles at:  
<http://cancerdiscovery.aacrjournals.org/content/3/3/338.full.html#related-urls>

**E-mail alerts** [Sign up to receive free email-alerts](#) related to this article or journal.

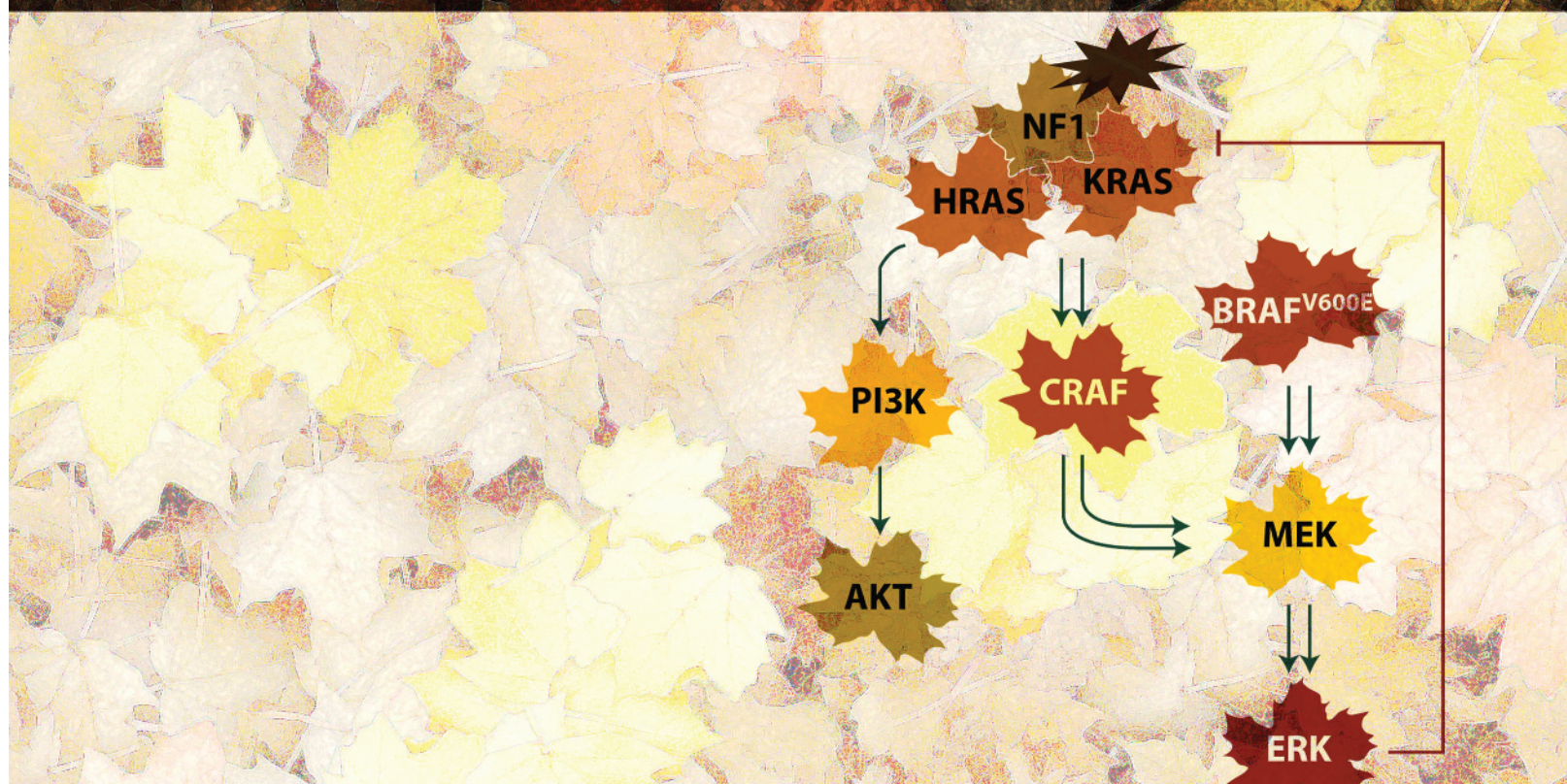
**Reprints and Subscriptions** To order reprints of this article or to subscribe to the journal, contact the AACR Publications Department at [pubs@aacr.org](mailto:pubs@aacr.org).

**Permissions** To request permission to re-use all or part of this article, contact the AACR Publications Department at [permissions@aacr.org](mailto:permissions@aacr.org).

RESEARCH ARTICLE

# Elucidating Distinct Roles for NF1 in Melanomagenesis

Ophélie Maertens<sup>1,3</sup>, Bryan Johnson<sup>1,3</sup>, Pablo Hollstein<sup>1,3</sup>, Dennie T. Frederick<sup>4</sup>, Zachary A. Cooper<sup>4</sup>, Ludwine Messiaen<sup>6</sup>, Roderick T. Bronson<sup>3</sup>, Martin McMahon<sup>7,8</sup>, Scott Granter<sup>2,3</sup>, Keith Flaherty<sup>4</sup>, Jennifer A. Wargo<sup>4</sup>, Richard Marais<sup>9</sup>, and Karen Cichowski<sup>1,3,5</sup>



**ABSTRACT**

*BRAF* mutations play a well-established role in melanomagenesis; however, without additional genetic alterations, tumor development is restricted by oncogene-induced senescence (OIS). Here, we show that mutations in the *NF1* tumor suppressor gene cooperate with *BRAF* mutations in melanomagenesis by preventing OIS. In a genetically engineered mouse model, *Nf1* mutations suppress *Braf*-induced senescence, promote melanocyte hyperproliferation, and enhance melanoma development. *Nf1* mutations function by deregulating both phosphoinositide 3-kinase and extracellular signal-regulated kinase pathways. As such, *Nf1/Braf*-mutant tumors are resistant to *BRAF* inhibitors but are sensitive to combined inhibition of mitogen-activated protein/extracellular signal-regulated kinase kinase and mTOR. Importantly, *NF1* is mutated or suppressed in human melanomas that harbor concurrent *BRAF* mutations. *NF1* ablation decreases the sensitivity of melanoma cell lines to *BRAF* inhibitors, and *NF1* is lost in tumors from patients following treatment with these agents. Collectively, these studies provide mechanistic insight into how *NF1* cooperates with *BRAF* mutations in melanoma and show that *NF1/neurofibromin* inactivation may have an impact on responses to targeted therapies.

**SIGNIFICANCE:** This study elucidates the mechanism by which *NF1* mutations cooperate with different *BRAF* mutations in melanomagenesis and shows that *NF1/neurofibromin* loss may desensitize tumors to *BRAF* inhibitors. *Cancer Discov*; 3(3); 338–49. ©2012 AACR.

See related commentary by Gibney and Smalley, p. 260.

**INTRODUCTION**

Oncogene-induced senescence (OIS) is an irreversible growth arrest that is triggered by a variety of oncogenic signals (1). This form of senescence functions as a protective response to aberrant cell signaling and has been shown to restrict the progression of benign lesions such as melanocytic nevi, lung adenomas, neurofibromas, and prostatic intraepithelial neoplasia (2). Several mechanisms have been proposed to underlie OIS, including excessive DNA damage (3–5), heterochromatin formation (6), negative feedback pathways (7, 8), and chemokine signaling (8–10). Notably, these mechanisms are not mutually exclusive, and it is likely that they cooperate to establish a senescence response in different tissues.

OIS has been shown to be important for restricting melanoma development in response to activating *BRAF* mutations (11, 12). *BRAF* is mutated in 50% to 70% of human melanomas (reviewed in ref. 13). The most frequent *BRAF* mutation (*BRAF*<sup>V600E</sup>)

results in a constitutively active kinase. Analysis of human lesions and mouse models has shown that *BRAF*<sup>V600E</sup> mutations drive the development of benign nevi (14–16). However, in the absence of additional mutations melanocytes within these nevi ultimately become senescent and do not progress to malignancy (11, 12, 15). Notably, a subset of genetic alterations found in human melanoma prevents *BRAF*-induced senescence, underscoring the importance of OIS as a mechanism of tumor suppression (15, 17). Nevertheless, we still do not have a complete mechanistic or genetic understanding of how OIS is bypassed in melanoma or more generally in cancer.

We have previously shown that oncogenic RAF triggers a potent negative feedback signaling network that suppresses RAS and that this feedback loop plays an important role in OIS *in vitro* (7). Specifically, in response to constitutively activated RAF and mitogen-activated protein/extracellular signal-regulated kinase kinase (MEK) proteins, RAS becomes suppressed because of the upregulation of several direct negative RAS regulatory proteins and the concomitant inactivation of positive RAS regulators (7). Moreover, RAF-induced RAS suppression substantially attenuates phosphoinositide 3-kinase (PI3K)/AKT signaling, which contributes to OIS in this setting (7). These observations raise the intriguing possibility that mutational events that promote RAS activation might play an important part in preventing RAF-induced senescence. If so, then mutations in such genes might be expected to cooperate with *BRAF* mutations in human cancer.

The *NF1* tumor suppressor gene encodes a RAS GTPase-activating protein (RAS GAP) neurofibromin, which negatively regulates RAS by catalyzing the hydrolysis of RAS-GTP to RAS-GDP (18). Accordingly, RAS and downstream effector pathways are aberrantly activated in *NF1*-deficient tumors (18–20). *NF1* is mutated in the familial cancer syndrome neurofibromatosis type I and has more recently been shown to be mutated or suppressed by proteasomal mechanisms in glioblastoma, lung cancer, and neuroblastoma (21–25); however, the full extent of *NF1* loss in sporadic tumorigenesis is unknown. Because of its

**Authors' Affiliations:** <sup>1</sup>Genetics Division, Department of Medicine, <sup>2</sup>Department of Pathology, Brigham and Women's Hospital; <sup>3</sup>Harvard Medical School; <sup>4</sup>Divisions of Surgical Oncology and Medical Oncology and Department of Dermatology, Massachusetts General Hospital; <sup>5</sup>Ludwig Center at Dana-Farber/Harvard Cancer Center, Boston, Massachusetts; <sup>6</sup>Department of Genetics, Medical Genomics Laboratory, University of Alabama at Birmingham, Birmingham, Alabama; <sup>7</sup>Cancer Research Institute; <sup>8</sup>Department of Cell and Molecular Pharmacology, Helen Diller Family Comprehensive Cancer Center, University of California, San Francisco, San Francisco, California; and <sup>9</sup>The Paterson Institute for Cancer Research, The University of Manchester, Manchester, United Kingdom

**Note:** Supplementary data for this article are available at *Cancer Discovery* Online (<http://cancerdiscovery.aacrjournals.org/>).

Current address for B. Johnson: Merrimack Pharmaceuticals Inc., Cambridge, Massachusetts.

**Corresponding Author:** Karen Cichowski, Brigham and Women's Hospital, 77 Avenue Louis Pasteur, NRB 0458C, Boston, MA 02115. Phone: 617-525-4722; Fax: 617-525-5801; E-mail: kcichowski@rics.bwh.harvard.edu

**doi:** 10.1158/2159-8290.CD-12-0313

©2012 American Association for Cancer Research.

direct effects on RAS and known involvement in melanocyte biology, we investigated a potential role for *Nf1* in melanomagenesis. Our studies reveal distinct mechanisms by which *Nf1* mutations cooperate with different *BRAF* mutations in melanomas. Moreover, we have found that *Nf1*/neurofibromin loss affects the therapeutic response to *BRAF* inhibitors.

## RESULTS

### *Nf1* Mutations Rescue the Inhibitory Effects of Constitutively Activated RAF

We previously showed that oncogenic *RAF* alleles potently suppress RAS and subsequent PI3K/AKT signaling and that this suppression is important for OIS in some settings (Fig. 1A; ref. 7). Because *Nf1* encodes a direct negative regulator of RAS, we reasoned that the effects of this feedback response might be counteracted by ablating *Nf1* expression. Wild-type and *Nf1*<sup>-/-</sup> mouse embryonic fibroblasts (MEF) were stably infected with a hydroxy-tamoxifen (4-OHT)-inducible, activated RAF construct (26). 4-OHT substantially suppressed RAS-GTP levels in wild-type cells, consistent with previous findings (Fig. 1B and C; ref. 7). However, RAF activation had minimal suppressive effects on RAS activity in *Nf1*<sup>-/-</sup> cells (Fig. 1B and C). Similar effects were also observed in cells in which *Nf1* expression was acutely ablated by short hairpin RNA (shRNA) sequences (Supplementary Fig. S1). Shortly

thereafter, AKT phosphorylation became substantially reduced in *Nf1* wild-type cells at both Ser473 and Thr308 (Fig. 1D and E); however, *Nf1* deficiency significantly ameliorated this suppression (Fig. 1D and E). It should be noted that even in the absence of *Nf1*, RAF partially inhibited AKT phosphorylation, consistent with the known involvement of several redundant negative feedback signals (7). Notably, *Nf1* loss caused a baseline activation of the PI3K/AKT pathway, as previously observed (Fig. 1D and E; refs. 19, 20), and therefore minimized the net suppressive effects on AKT. Most importantly, however, RAF activation exerted differential effects on proliferation in wild-type and *Nf1*-mutant cells. Consistent with previous observations, oncogenic RAF caused a potent and irreversible growth arrest in *Nf1* wild-type MEFs (Fig. 1F; refs. 27, 28). However, RAF activation did not suppress the proliferation of *Nf1*-deficient cells (Fig. 1G), showing that RAS suppression is a critical mediator of this inhibitory response.

### Compound Mutations in *Nf1* and *Braf* Promote Melanocyte Hyperproliferation In Vivo

To investigate the potential cooperativity of *Nf1* and *RAF* mutations in a relevant tumorigenic setting, we generated a mouse model to evaluate the effects of *Nf1* loss in the presence of activating *Braf* mutations. As noted previously, *BRAF* is mutated in 50% to 70% of human melanomas (13). On the basis of our *in vitro* findings and the fact that neurofibromin

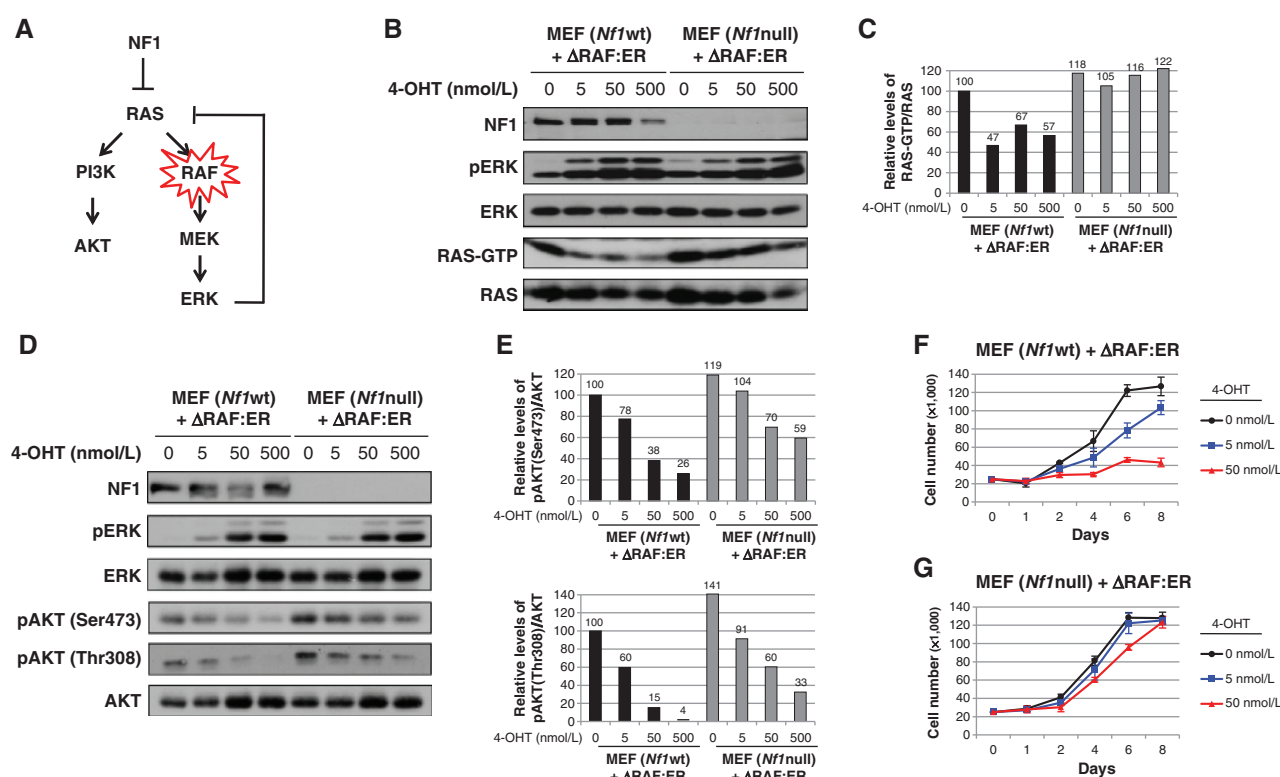


**Figure 1.** *Nf1* mutations rescue the inhibitory effects of activated RAF. **A**, model of negative feedback pathway and the role that *Nf1* could play in alleviating suppression. **B**, *Nf1* wild-type (wt) and null MEFs expressing an inducible RAF construct (ΔRAF:ER) were treated with the indicated concentrations of 4-OHT for 24 hours. Immunoblots of total cell lysates evaluating phospho-ERK, total ERK, RAS, and neurofibromin (NF1) are shown. RAS-GTP levels were assessed using a RAS pull-down assay and are quantified relative to total RAS levels in **C**. **D**, immunoblots evaluating phospho-ERK and phospho-AKT in total cell lysates from cells treated with 4-OHT for 72 hours are shown. Relative phospho-AKT (Ser473) and phospho-AKT (Thr308) levels are quantified in **E**. **F**, proliferation curve of *Nf1* wild-type, and **G**, *Nf1* null MEFs expressing the inducible RAF construct after exposure to increasing concentrations of 4-OHT.

plays a well-established role in melanocytes (29), we evaluated the potential cooperativity of *Braf* and *Nf1* mutations in the context of melanomagenesis.

Mice carrying a conditional inactivating mutation in *Nf1* (*Nf1*<sup>fl/fl</sup> mice; ref. 30) were crossed to mice with a conditional activating mutation in *Braf* (*Braf*<sup>CA/+</sup> mice; ref. 31). These animals were then crossed to a transgenic mouse strain harboring a tamoxifen-inducible Cre recombinase–estrogen receptor fusion transgene that is under the control of the melanocyte-specific tyrosinase promoter, designated *Tyr::CreER<sup>T2</sup>* (32). Activation of CreER by tamoxifen in *Tyr::CreER<sup>T2</sup>; Braf<sup>CA/+</sup>; Nf1<sup>fl/fl</sup>* mice leads to melanocyte-specific conversion of *Braf<sup>CA</sup>* to *Braf<sup>V600E</sup>* and the conversion of the *Nf1<sup>fl/fl</sup>* alleles to *Nf1* null alleles. Six genetic cohorts of animals were generated to evaluate the effects of *Braf* activation in the presence and absence of *Nf1*.

Mice were treated topically with tamoxifen 2 to 3 months after birth, as previously described (15). After 4 to 5 weeks, significant darkening of the tails, ears, eyelids, perianal regions, and paws was observed in the *Tyr::CreER<sup>T2</sup>; Braf<sup>CA/+</sup>; Nf1<sup>fl/fl</sup>* mice, as compared with all other genotypes (Fig. 2A and B). Whereas *Tyr::CreER<sup>T2</sup>; Braf<sup>CA/+</sup>* animals exhibited subtle hyperpigmentation, the skin hyperpigmentation in the *Tyr::CreER<sup>T2</sup>; Braf<sup>CA/+</sup>; Nf1<sup>fl/fl</sup>* mice became dramatically more pronounced over time and was concurrent with visible thickening of the respective

tissues (Fig. 2A and B). The histopathologic features of these lesions were consistent with expansion of the dermis, the skin layer in which murine melanocytes reside, and massive melanin deposition (Fig. 2C). An increased number of cells expressing the melanocyte marker S100 were observed, confirming excessive melanocyte hyperproliferation in *Tyr::CreER<sup>T2</sup>; Braf<sup>CA/+</sup>; Nf1<sup>fl/fl</sup>* mice, as compared with the *Braf<sup>CA/+</sup>* genotype (Fig. 2C). Importantly, we found that deep dermal lesions derived from control *Tyr::CreER<sup>T2</sup>; Braf<sup>CA/+</sup>* mice stained positive for senescence associated-β-galactosidase (SA-β-gal; Fig. 2D, top), as has been shown in human nevi (12) and in lesions within the *Braf<sup>V600E</sup>*-driven mouse model described by Dhomen and colleagues (15). However, senescence was not observed in *Tyr::CreER<sup>T2</sup>; Braf<sup>CA/+</sup>; Nf1<sup>fl/fl</sup>* mice (Fig. 2D, bottom). These results are consistent with our cellular studies and indicate that mutations in *Nf1* prevent *Braf*-induced senescence of melanocytes in mice, thereby rescuing the proliferative restriction and triggering excessive proliferation.

PI3K is a well-known effector of RAS (33). We and others have previously shown that *NF1* loss triggers activation of the PI3K/AKT/mTOR pathway through RAS (19, 20, 34). Moreover, *Nf1* mutations minimized the suppressive effects of *Braf* mutations on this pathway (Fig. 1D and E). Notably, we found that the PI3K inhibitor GDC-0941 prevented melanocytic hyperplasia in *Tyr::CreER<sup>T2</sup>; Braf<sup>CA/+</sup>; Nf1<sup>fl/fl</sup>* mice (Fig. 2E),

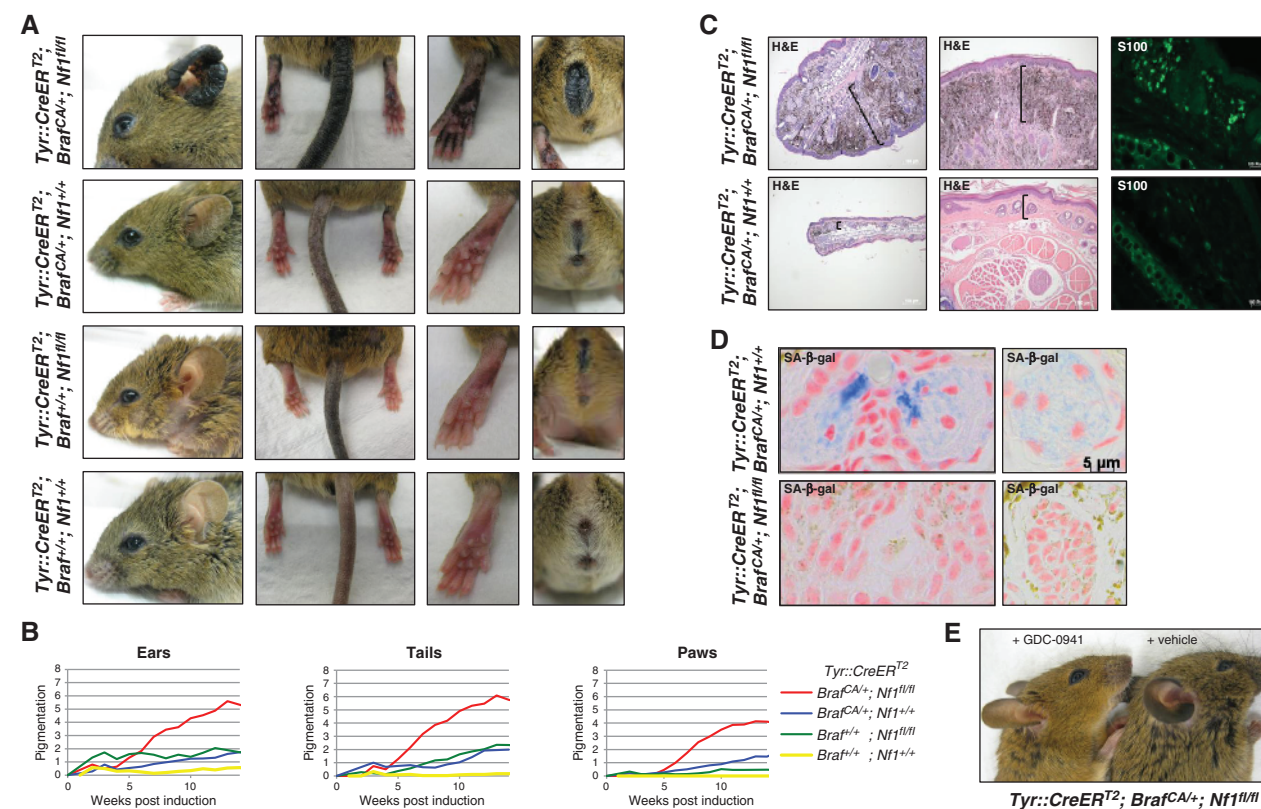


**Figure 2.** *Nf1* and *Braf* mutations cooperate *in vivo* and lead to enhanced melanocyte proliferation. **A**, phenotype of mice with the indicated genotypes 7 months after *Tyr::CreER<sup>T2</sup>* induction. **B**, quantification of pigmentation phenotype of different genotypes over time following *Tyr::CreER<sup>T2</sup>* induction. **C**, histologic images of ears (left) and tails (middle) from mice with the specified genotypes 9 months after tamoxifen treatment. Brackets indicate dermis in respective tissues at same magnification. S100 expression was evaluated by immunofluorescent staining (right). **D**, sections of ear stained for eosin and SA-β-gal (light blue) from tamoxifen-treated *Tyr::CreER<sup>T2</sup>; Braf<sup>CA/+</sup>; Nf1<sup>fl/fl</sup>* (top) and *Tyr::CreER<sup>T2</sup>; Braf<sup>CA/+</sup>; Nf1<sup>fl/fl</sup>* (bottom) mice. Note the blue staining and cell morphology differences. **E**, *Tyr::CreER<sup>T2</sup>; Braf<sup>CA/+</sup>; Nf1<sup>fl/fl</sup>* mice were treated daily with the PI3K inhibitor GDC-0941 (150 mg/kg) or vehicle for 8 weeks after *Tyr::CreER<sup>T2</sup>* induction. The hyperpigmentation phenotype was prevented by GDC-0941 treatment.

showing that *Nf1* loss was mediating its effects in melanocytes, in part, by permitting or enhancing the activation of this pathway.

### **Nf1 and Braf Mutations Cooperate to Promote Melanomas in Mice**

If OIS does in fact restrict tumor development, then *Braf/Nf1*-mutant mice would be expected to be more prone to developing melanomas. It has been previously reported that a subset of *Braf<sup>V600E</sup>* mice develop melanomas, presumably owing to the stochastic acquisition of additional genetic alterations (15). Consistent with this observation 22% (6 of 27) of the *Braf<sup>V600E</sup>* mice in our cohort developed melanomas; however, 57% (16 of 28) of the *Tyr::CreERT<sup>2</sup>; Braf<sup>CA/+</sup>; Nf1<sup>fl/fl</sup>* mice developed melanomas ( $P = 0.008$ ;  $\chi^2$  test; Fig. 3A–E). One *Braf/Nf1*-mutant mouse developed 2 melanomas, an event never observed in *Braf*-mutant animals; however, melanomas from both genotypes grew at similar rates. These observations support the hypothesis that *Nf1* loss prevents *Braf*-induced senescence *in vivo* and therefore plays a role early in tumor development rather than in progression. However, effects on metastasis could not be evaluated in this model, as animals from both genotypes needed

to be euthanized because of primary tumor size. Although pigmented melanocytes were occasionally observed on the exterior, these melanomas were typically hypopigmented (Fig. 3B). All *Braf/Nf1* tumors displayed histologic and cytologic features typical of malignant melanomas. Tumors were highly cellular, with most showing a fascicular growth pattern (Fig. 3C). The degree of pleomorphism was variable. The majority of the tumor cells were amelanotic; however, many tumors showed occasional clusters of pigmented cells and pigment-containing macrophages (melanophages; Fig. 3C, right). All tumors involved the dermis as well as subcutaneous soft tissue, and ulceration of the tumor surface was seen in the majority of cases. Tumors expressed both S100 (Fig. 3D) and microphthalmia-associated transcription factor (MITF; Fig. 3E), 2 markers typically used to diagnose human melanomas. Melanomas from both genotypes were further evaluated by immunoblot (Fig. 3F). One tumor that developed in *Tyr::CreERT<sup>2</sup>; Braf<sup>CA/+</sup>; Nf1<sup>fl/fl</sup>* mice did not efficiently excise *Nf1*. However, in general, higher levels of phospho-AKT were typically observed in *Braf/Nf1*-mutant versus *Braf*-mutant tumors (Fig. 3F and G), consistent with the observation that *Nf1* mutations enhance PI3K/AKT activation and contribute to tumorigenesis, in part via this pathway (refs. 19, 20, 34; Fig. 2E).

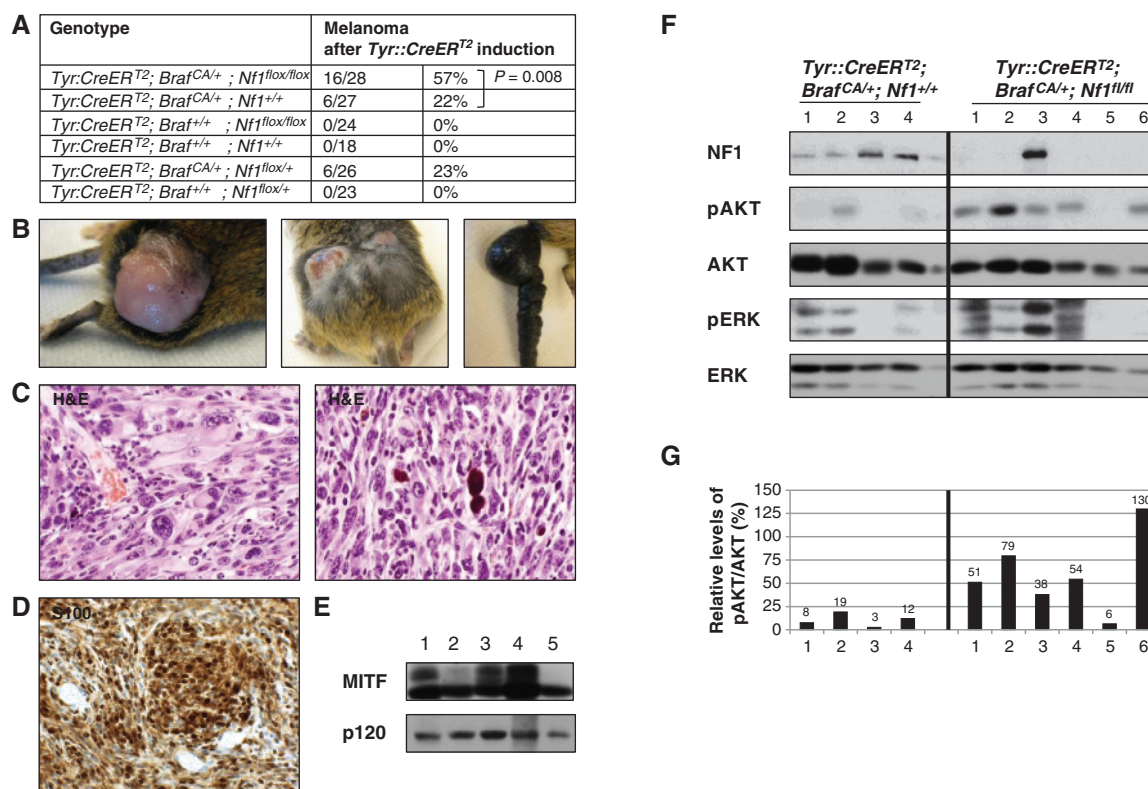


**Figure 3.** *Nf1* and *Braf* mutations cooperate to promote melanomagenesis in mice. **A**, genotypes and tumor phenotypes of experimental animals and control groups. **B**, pictures showing tumors from tamoxifen-treated *Tyr::CreERT<sup>2</sup>; Braf<sup>CA/+</sup>; Nf1<sup>fl/fl</sup>* mice. Note the pigmented area on the surface of the tumor (left), the presence of more than one lesion (middle), and the remarkable thickening of the tail (right). **C** and **D**, representative histologic images ( $\times 400$  magnification) of tumors from tamoxifen-induced *Tyr::CreERT<sup>2</sup>; Braf<sup>CA/+</sup>; Nf1<sup>fl/fl</sup>* mice. **C**, tumor sections are stained with H&E. Tumors show marked cytologic atypia and pleomorphism, including bizarre cells with irregular chromatin distribution and irregular nuclear outlines (left). Occasionally, melanophages containing extensive brown pigment were observed (right). **D**, the vast majority of neoplastic cells stain positive for S100. **E**, MITF protein expression in primary tumor tissue from tamoxifen-treated *Tyr::CreERT<sup>2</sup>; Braf<sup>CA/+</sup>; Nf1<sup>fl/fl</sup>* mice was confirmed by immunoblotting. **F**, protein levels of NF1, phospho-AKT, and phospho-ERK in distinct tumors from tamoxifen-induced *Tyr::CreERT<sup>2</sup>; Braf<sup>CA/+</sup>; Nf1<sup>+/+</sup>* (left) and *Tyr::CreERT<sup>2</sup>; Braf<sup>CA/+</sup>; Nf1<sup>fl/fl</sup>* (right) mice, as determined by immunoblotting. Relative phospho-AKT levels are quantified in **G**.

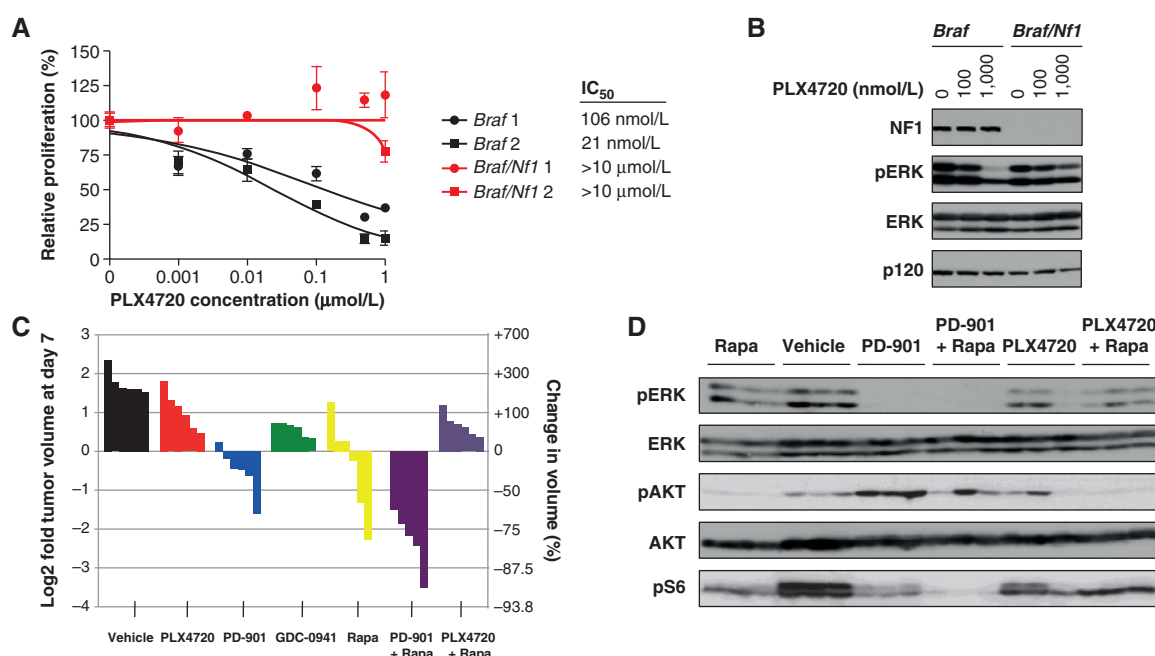


**Figure 4.** *Nf1* mutations desensitize mouse melanomas to BRAF inhibitors. **A**, dose-sensitivity curves for PLX4720 are shown for 2 independently derived cell lines from *Braf*-mutant (black) and *Braf/Nf1*-mutant (red) melanomas. **B**, pharmacodynamic analysis of phospho-ERK in *Braf* and *Braf/Nf1*-mutant cells in vitro after a 24-hour incubation with 0, 100, and 1,000 nmol/L PLX4720. **C**, waterfall plot depicting tumor growth of *Braf/Nf1*-mutant allografts after 7 days of treatment with vehicle (black), PLX4720 (red), PD0325901 (PD-901, blue), GDC-0941 (green), rapamycin (Rapa, yellow), PD0325901 + rapamycin (purple), and PLX4720 + rapamycin (violet). Each bar represents a different tumor. Both *Braf/Nf1*-mutant cell lines shown in **A** were injected into 3 mice each, resulting in a total of 6 tumors per treatment arm. **D**, *in vivo* pharmacodynamic analysis of phospho-ERK, phospho-AKT, and phospho-S6 in *Braf/Nf1*-mutant allografts treated with rapamycin (Rapa), vehicle, PD0325901 (PD-901), PD0325901 + rapamycin, PLX4720, and PLX4720 + rapamycin. Lysates were prepared from tumor tissues that were harvested 2 hours post administration of the respective treatment from 3 tumors shown in **C**. pS6, ribosomal protein S6.

### Nf1 Mutations Desensitize Melanomas to BRAF Inhibitors

The mutant BRAF selective inhibitor PLX4032 (vemurafenib; Plexxikon/Roche) promotes the regression of human melanomas that harbor activating *BRAF* mutations and has been approved for treating human melanomas (35). To investigate the sensitivity of melanomas harboring compound mutations in *Braf* and *Nf1* to BRAF inhibitors and other targeted agents, we first isolated cells from *Braf* and *Braf/Nf1*-mutant tumors. As expected, cells from 2 independently derived *Braf*-mutant melanomas were sensitive to the PLX4032 analog, PLX4720 (Fig. 4A). However, cells from *Braf/Nf1*-mutant tumors were insensitive to this agent (Fig. 4A; IC<sub>50</sub> > 10  $\mu\text{mol/L}$ ). Biochemical studies confirmed that increasing concentrations of PLX4720 effectively suppressed phospho-extracellular signal-regulated kinase (ERK) levels in *Braf*-mutant cells (Fig. 4B). Notably, however, phospho-ERK was not as effectively suppressed in *Braf/Nf1*-mutant cells (Fig. 4B).

Next, we evaluated sensitivity to these agents *in vivo*. Whereas allografts from several independent *Braf/Nf1*-mutant melanomas were readily established, cells from *Braf*-mutant mouse melanomas never successfully grew as allografts. As such, we focused on using *Braf/Nf1*-mutant allografts to determine whether we could identify a more effective therapy for these genetically distinct tumors. Two weeks after injection, when tumors were growing in log phase, mice were randomly divided into different treatment groups. Similar to our *in vitro* analysis, *Braf/Nf1*-mutant melanomas were relatively

insensitive to PLX4720 (Fig. 4C, red) and phospho-ERK was not efficiently inhibited in tumors *in vivo* (Fig. 4D). This finding is consistent with the observation that induction of tumor regression by PLX4032 requires almost complete suppression of ERK signaling (36). In contrast, these tumors were more sensitive to the MEK inhibitor PD0325901 (Fig. 4C, blue), which effectively suppressed phospho-ERK *in vivo* (Fig. 4D). Together with our *in vitro* studies, this insensitivity suggests that neurofibromin loss may enhance ERK activity via a BRAF-independent mechanism, which will be further discussed later.

Because our *in vivo* experiments showed that melanocyte hyperproliferation in *Tyr::CreER*<sup>T2</sup>; *Braf*<sup>CA/+</sup>; *Nf1*<sup>flox/flox</sup> mice could be rescued by the PI3K inhibitor GDC-0941, we evaluated the effects of GDC-0941 on tumor growth and found that it had a slight growth-suppressive effect on these melanomas (Fig. 4C, green). However, given that mTOR has been shown to be an important effector in *Nf1*-mutant tumors, we also assessed the mTOR inhibitor rapamycin (20, 34, 37). Rapamycin had a more pronounced effect than GDC-0941, but more importantly it synergized with PD0325901 to promote tumor regression (Fig. 4C, purple). In contrast, rapamycin did not promote tumor regression when combined with PLX4720 (Fig. 4C, violet). Taken together, these results suggest that *Nf1* mutations can desensitize *Braf*-mutant melanomas to PLX4720. On the basis of the biochemical function of neurofibromin and the preclinical data presented here, therapies aimed at targeting both MEK and mTOR may

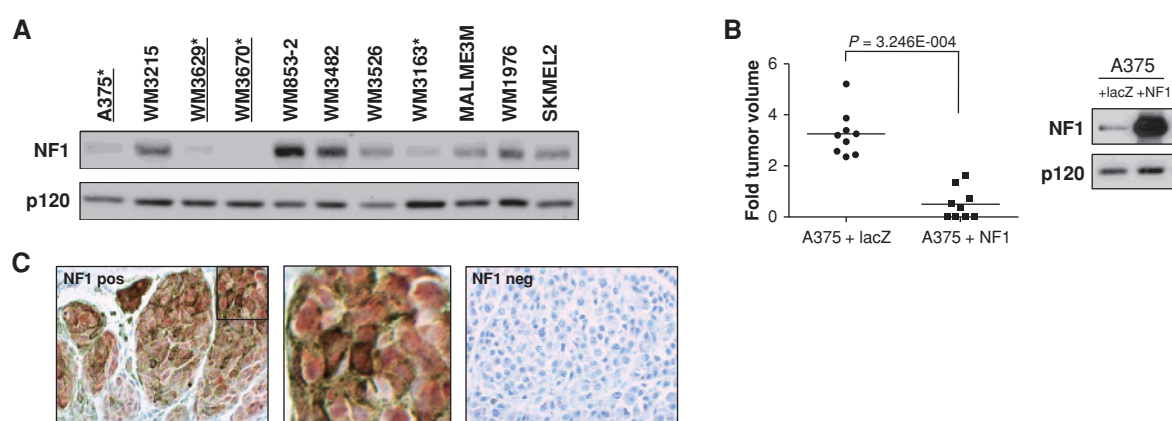


**Figure 5.** NF1 protein expression in human melanomas. **A**, NF1 protein levels in a panel of 11 human melanoma cell lines, as determined by immunoblotting. Four lines (with asterisks) exhibit low or no NF1 expression. Three lines (underlined) harbor NF1 mutations. **B**, NF1 reconstitution in A375 cells potently suppresses the growth of xenografts in mice. Tumor size is shown on left, protein expression on right. **C**, tissue microarray analysis of NF1 in human malignant and metastatic melanomas. Positive NF1 staining in nevus is shown on left. A magnification of the inset box is shown in the middle. Negative NF1 staining in human melanoma is shown on the right.

represent an alternative therapeutic approach for *BRAF/NF1*-mutant tumors.

### NF1 Is Suppressed and/or Mutated in Human Melanoma

Given these compelling mouse phenotypes, we next investigated whether *NF1* is lost or mutated in human melanomas. Like P53, neurofibromin can be inactivated by both genetic and proteasomal mechanisms (23). We first evaluated neurofibromin expression in a panel of melanoma cell lines. Four of 11 cell lines exhibited little or no neurofibromin expression (Fig. 5A). Sequence analysis confirmed that 3 of these cell lines harbored loss-of-function mutations in the *NF1* gene (Supplementary Table S1). It should be noted that 2 of the *NF1* alterations (p.K1290K in A375 cells and p.K2307K in WM3670 cells) abolish splice donor sites (c.3870G>A and c.6921G>A, respectively), result in defective splicing, and disrupt the *NF1* transcript. Sequence analysis of the cDNA of *NF1* enabled the detection of these aberrant splicing events; however, both *NF1* mutations may have been categorized as “non-deleterious” silent alterations using exome sequencing approaches. We then mined publicly available databases and identified numerous additional *NF1* mutations in human cell lines (Supplementary Table S1). Analysis of primary melanomas also confirmed the presence of somatic *NF1* mutations (Supplementary Table S2). In many, but not in all, cases *BRAF* mutations were also present. These findings suggest that *NF1* mutations can cooperate with activating *BRAF* mutations, but they may also play a broader role in melanomagenesis. Interestingly, however, although we expected to find coincidental mutations with *BRAFV600E*, we also observed *NF1* mutations in cells that harbored inactivating *BRAF* mutations (Supplementary Table S1), a point that will be discussed later.

To complement the mouse modeling studies and confirm a functional role for *NF1* inactivation in human melanomas, we reconstituted neurofibromin in A375 cells, which harbor compound *NF1* and *BRAFV600E* mutations. Full-length neurofibromin expression potently suppressed the growth of xenografts in mice ( $P = 3.246E-004$ ; Mann–Whitney  $U$  test),

consistent with the notion that *NF1* inactivation plays a causal role in tumor development (Fig. 5B). As noted earlier, the NF1 tumor suppressor is frequently inactivated by proteasomal mechanisms in human cancer (23). As such, mutational analysis may underestimate the frequency of *NF1/neurofibromin* loss in tumors. Therefore, we conducted immunohistochemical analysis on human melanoma tumor arrays. No visible neurofibromin expression was observed in 15% (6 of 39) of melanomas and 18% (6 of 34) of metastatic melanomas (Fig. 5C and Supplementary Table S3). It should be noted that only a complete absence of staining was scored as negative in this analysis. Therefore, excessive but incomplete neurofibromin destruction was not considered, but could still play a role in tumor development.

### NF1 Loss and BRAF Inhibitors in Human Tumors

Preclinical studies in mouse tumors suggested that *Nf1* loss can desensitize *Braf*-mutant melanomas to *BRAF* inhibitors. To evaluate this possibility in human tumors, we genetically ablated neurofibromin expression with lentiviral shRNA sequences in human melanoma cell lines and found that *NF1* suppression decreased the sensitivity of WM3526 cells to PLX4720 by 11-fold (Fig. 6A and Supplementary Fig. S2). As noted previously, A375 cells harbor a loss-of-function *NF1* mutation and express very low levels of neurofibromin. Because these cells remain somewhat sensitive to *BRAF* inhibitors, we further reduced neurofibromin expression with shRNA sequences and found that *NF1* suppression also decreased the sensitivity of these cells to *BRAF* inhibitors (Fig. 6B and Supplementary Fig. S2). It should be noted that although the acute ablation of *NF1* in established melanoma cell lines desensitized these cells to PLX4720, tumors that naturally developed in the absence of *Nf1* were much more resistant to this agent. We hypothesize that this difference may reflect inherent differences in preexisting signaling networks and/or cooperating mutations in these established tumor cells, which did not evolve in the absence of *NF1*. Nevertheless, consistent with observations in mouse tumors, PLX4720 was much less effective at suppressing phospho-ERK in cells in which *NF1* was

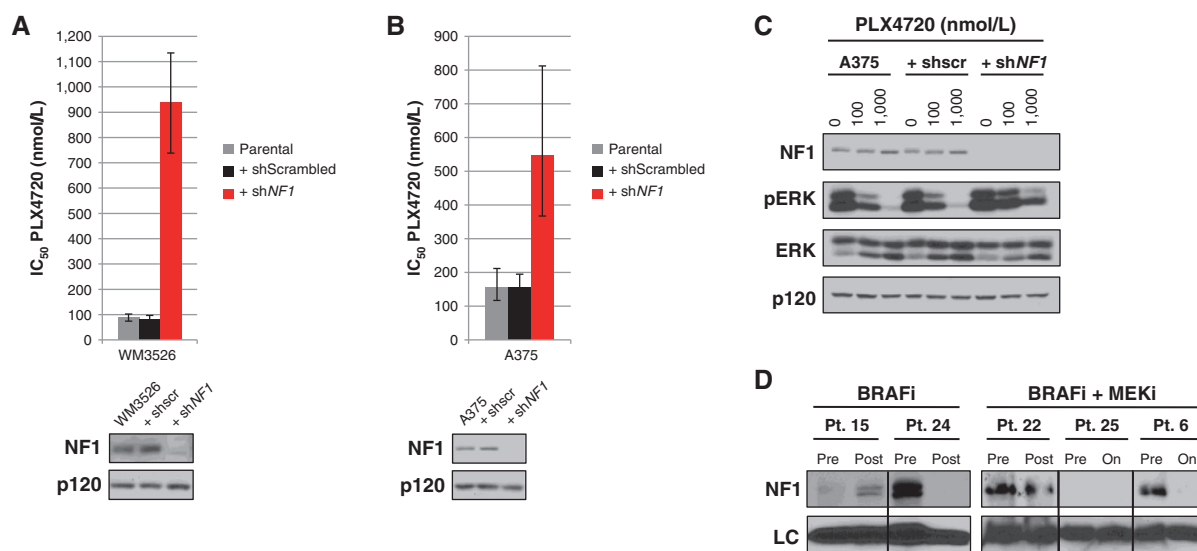


**Figure 6.** NF1 levels mediate sensitivity to BRAF inhibition. **A**, bar graph representing IC<sub>50</sub> values for PLX4720 in the BRAF<sup>V600E</sup>-mutant melanoma cell line WM3526 in the absence or presence of a shRNA specific for NF1. The doubling time of these cells did not change in the presence of shRNA sequences. **B**, similar graph representing IC<sub>50</sub> values for PLX4720 in the BRAF<sup>V600E</sup>-mutant melanoma cell line A375. **C**, pharmacodynamic analysis of phospho-ERK in A375 cells, with or without residual NF1 expression, after a 24-hour incubation with 0, 100, and 1,000 nmol/L PLX4720. **D**, NF1 protein levels in tumor biopsy specimens from patients (Pt.) before (Pre) and after (Post) treatment with a BRAF inhibitor (BRAFi; vemurafenib) or combined BRAF/MEK inhibitors (BRAFi + MEKi; dabrafenib + trametinib). Where indicated, samples were collected from specimens from relapsed biopsies (Post) or from residual tumor tissue. The word "On" refers to patients still on treatment. Total levels of glyceraldehyde-3-phosphate dehydrogenase (GAPDH; BRAFi samples) and HSC70 (BRAFi + MEKi samples) served as loading controls (LC). Scr, scrambled.

ablated, indicating that NF1 loss promotes BRAF-independent ERK signaling in these tumor cells as well (Fig. 6C).

Finally, we were able to obtain frozen tissue from 5 sets of pre- and posttreatment tumor biopsy specimens from patients treated with a BRAF inhibitor (vemurafenib) or combined BRAF/MEK inhibitors (dabrafenib + trametinib). Notably, 2 of 5 tumors expressed very little or no neurofibromin before treatment, consistent with the observation that NF1/neurofibromin is lost or suppressed in human melanomas at a relatively frequent rate (Fig. 6D). However, in 2 of the remaining 3 tumors in which neurofibromin was robustly expressed before treatment, neurofibromin was no longer expressed in tumors following treatment (Fig. 6D). Taken together with preclinical studies in the mouse model and genetic studies in human melanoma cell lines, these observations further support the hypothesis that NF1/neurofibromin suppression may play an important role in mediating resistance to BRAF inhibitors. Notably, in glioblastoma, neurofibromin seems to be more frequently lost by proteasomal mechanisms (23). Therefore, future studies aimed at assessing NF1/neurofibromin loss in response to therapies will likely require analysis of both protein expression and genetic alterations.

### NF1 Mutations Cooperate with BRAF Mutations by Activating Both K- and HRAS

Our central hypothesis is that loss of NF1 alleviates the suppression of RAS imposed by activated BRAF. To identify the RAS isoforms that are critically regulated by neurofibromin in melanomas, we conducted both gain- and loss-of-function studies. In melanoma cells that retain neurofibromin expression, RNA interference (RNAi)-mediated suppression of neurofibromin resulted in the activation of H- and KRAS but not

NRAS (Fig. 7A). Conversely, reconstituting melanoma cell lines with an active neurofibromin fragment suppressed H- and KRAS activity but not NRAS activity (Fig. 7B). Finally, shRNA-mediated suppression of either H- or KRAS suppressed the ability of NF1-deficient melanoma cells harboring an active BRAF mutation to proliferate and form colonies in soft agar, whereas NRAS-specific shRNA sequences had no effect (Fig. 7C–E). These results suggest that neurofibromin loss/suppression activates H- and KRAS in melanomas and that both of these isoforms are critical for the tumorigenicity of these cancer cells.

As shown in Supplementary Table S1, NF1 mutations were also detected in cells that harbored inactivating BRAF mutations. Although the kinase activity of these BRAF proteins is compromised, they have been proposed to function as scaffolds that translocate CRAF to the membrane and promote CRAF activation downstream of KRAS (38). Notably, the oncogenic effects of these mutants are significantly enhanced in the presence of KRAS<sup>G12D</sup> (38). Similarly, an NF1 mutation might be expected to function as an alternative mechanism of activating KRAS, and also potentiate the effects of these BRAF mutants. To evaluate the contribution of RAS isoforms in human melanomas, we examined WM3629 cells. Interestingly, in addition to harboring the kinase-dead BRAF<sup>D594G</sup> mutation and an NF1 deletion, this cell line also possesses an activating NRAS<sup>G12D</sup> mutation (39, 40). The WM3629 line similarly harbors an inactivating BRAF mutation, as well as NF1 and NRAS<sup>G12D</sup> mutations (39, 40). Consistent with the presence of these mutations and our previous observations, NRAS, KRAS, and HRAS are all activated in WM3629 cells. Moreover, shRNA-mediated ablation of all 3 RAS isoforms—H-, K-, and NRAS—suppressed the ability of WM3629 cells to proliferate and form colonies in soft agar (Fig. 7F–H). These

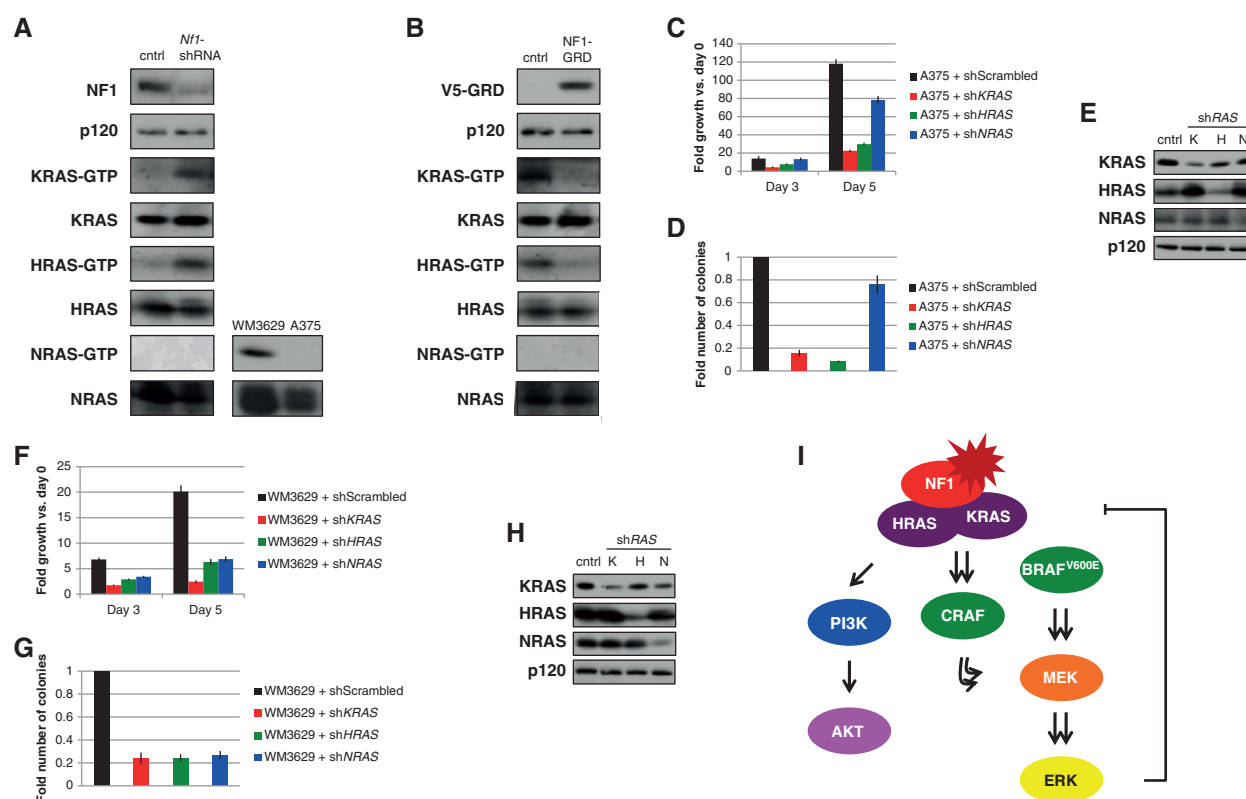


**Figure 7.** NF1 critically regulates KRAS and HRAS in melanomas. **A**, left, in WM1976 melanoma cells that retain NF1 expression, RNAi-mediated suppression of NF1 results in the activation of H- and KRAS, but not NRAS. Bottom right, NRAS-GTP assay confirming that NRAS is active in melanoma cells with an activating NRAS mutation (WM3629), but not in melanoma cells wild-type for NRAS (A375). **B**, ectopic expression of the catalytically active NF1 fragment (GRD) suppresses H- and KRAS, but not NRAS, activity in melanoma cells (MALME3M). RAS-GTP levels were assessed using a RAS pull-down assay. Immunoblots on total cell lysates are shown. **C**, shRNA-mediated suppression of H- or KRAS, but not NRAS, suppresses the ability of A375 cells to proliferate and **(D)** form colonies in soft agar. **E**, confirmation of RAS isoform-specific knockdown by shRNAs in A375 cells. **F**, shRNA-mediated suppression of H-, K-, and NRAS suppresses the ability of WM3629 cells to proliferate and **(G)** form colonies in soft agar. **H**, confirmation of RAS isoform-specific knockdown by shRNAs in WM3629 cells. **I**, model showing the distinct roles of NF1 in melanomagenesis.

results further show that neurofibromin critically regulates H- and KRAS in melanomas and suggest that in the presence of NRAS mutations all 3 RAS isoforms cooperate with inactivating BRAF mutations to promote tumorigenesis.

## DISCUSSION

This study establishes several distinct roles for *NF1* in melanomagenesis. First, our data suggest that in the presence of activating *Braf* mutations, *Nf1* loss prevents *Braf*-induced senescence of melanocytes. In mice, this results in excessive melanocyte hyperproliferation and ultimately enhances melanoma development. Importantly, *NF1* mutations cooccur with activating *BRAF* mutations in human melanomas, and neurofibromin reconstitution potently suppresses the growth of human melanoma cells as xenografts, further supporting a causal role for *NF1* loss in melanomagenesis. However, we have found that *NF1* mutations can also cooperate with inactivating *BRAF* mutations in melanomas. Although these *BRAF* mutations are less common, in this setting we found that *NF1* mutations cooccur with NRAS mutations and that all 3 RAS isoforms are required for the tumorigenic properties of these cells. Thus, *NF1* mutations can contribute to melanoma development in at least 2 genetic settings via distinct mechanisms.

We also found that in the context of activating *BRAF* alleles *NF1* mutations contribute to tumorigenesis, in part by promoting activation of the PI3K/AKT/mTOR pathway. Notably, the *PTEN* tumor suppressor is commonly mutated or lost in human melanomas (41). Mouse modeling studies and human tumor analysis suggest that *BRAF* and *PTEN* mutations cooperate in melanomagenesis (14). More recently, *PTEN* loss has been shown to prevent *BRAF*-induced senescence in mice and in human melanocytes, further supporting the notion that coactivation of these pathways is important for preventing OIS (17). Our data show that *NF1* loss is another important mechanism by which the PI3K pathway can become activated in melanomas. It should be noted, however, that *NF1* and *PTEN* mutations do not seem to be mutually exclusive in melanomas. Moreover, we have found that *NF1* loss also results in the activation of multiple RAS isoforms and potentiates ERK activation independent from activating *BRAF* mutations. Taken together, these observations suggest that *NF1* loss contributes to melanomagenesis by enhancing the activation of both PI3K and ERK signaling, which may be important in the context of selecting effective therapies (model presented in Fig. 7I).

Several mechanisms have been reported to mediate the resistance of *BRAF*-mutant melanomas to *BRAF* inhibitors

(42–46). Additional mechanisms are likely to be discovered, and currently one prevalent mechanism of resistance has not emerged. We have shown that *Nf1* mutations confer resistance to PLX4720 in *Braf*-mutant mouse melanomas; however, these tumors are sensitive to combined MEK/mTOR inhibitors. Importantly, RNAi-mediated *NF1* suppression also decreases the sensitivity of human melanoma cell lines to BRAF inhibitors, and, most notably, *NF1*/neurofibromin is lost in a subset of relapsing and residual tumors from patients exposed to BRAF inhibitors. The observation that *NF1*/neurofibromin is also mutated or lost in some naïve primary tumors is consistent with the hypothesis that *NF1* inactivation may contribute to both *de novo* and acquired resistance. However, although *NF1* mutations can be detected in human melanomas, the true frequency of NF1 loss may be difficult to assess, because like PTEN and P53, the NF1 protein is frequently inactivated by proteasomal destruction (23). Immunohistochemical analysis of tumor microarrays indicates that neurofibromin expression is completely absent in 15% to 18% of melanomas; however, a more quantitative evaluation of protein levels may be required to accurately evaluate its expression or suppression before and after drug treatment. To date, much of the resistance to BRAF inhibitors seems to be driven by events that activate ERK through mechanisms that circumvent or decrease dependency on BRAF. However, aberrant activation of the PI3K/AKT pathway has also been implicated in resistance to BRAF inhibitors (46–48). In this respect, NF1 (loss) is uniquely poised, as it activates the ERK pathway through its effects on KRAS and HRAS and at the same time enhances PI3K/AKT/mTOR signaling.

## METHODS

### *Cell Culture Techniques, Infections, and Proliferation Curves*

Wild-type and *Nf1* null MEFs were generated as described (49). Cells were stably infected with a pBabe retroviral vector containing the 4-OHT-inducible estrogen receptor RAF-1 (ΔRAF:ER) construct (28). This construct is an estrogen receptor-RAF-1 fusion molecule, and contains the ligand-binding domain of the estrogen receptor fused to the activated RAF kinase domain of RAF-1. Cells were split to an equal density 16 hours before harvesting in Dulbecco modified Eagle medium (DMEM) containing 1% fetal calf serum (FCS) and different concentrations of 4-OHT (0, 5, 50, or 500 nmol/L). For proliferation studies, cells were seeded at a density of  $25 \times 10^4$  in a 12-well format in DMEM containing 10% FCS and different concentrations of 4-OHT (0, 5, and 50 nmol/L). Cells were counted the day after plating and every other day after, until uninduced cells reached confluence. Media containing fresh 4-OHT were changed every 48 hours. The melanoma cell lines were obtained from the American Type Culture Collection and the Garraway laboratory (46). No additional authentication was done by the authors. All melanoma cell lines were grown in RPMI medium supplemented with 10% FCS, penicillin, and streptomycin. For dose-response curves, cells were seeded in triplicate in a 6-well format. Cells were counted the day after plating, when PLX4720 (Calbiochem) was added, as well as after 3 days, when dimethyl sulfoxide (DMSO)-treated cells reached confluence. To allow comparison of the IC<sub>50</sub> between cell lines, growth inhibition was calculated at 5 population doublings for every cell line. Neurofibromin activity was reconstituted using the previously described NF1-GAP-related domain (GRD) construct (20) or an expression vector containing full-

length *NF1* cDNA. Neurofibromin expression was abolished using shRNAs specific to *NF1* (20).

### *Preparation of Protein Lysates and Western Blotting*

RAS-GTP levels were detected using a RAS activation assay, following the manufacturer's instructions (EMD Millipore). Tumor lysates were homogenized and extracted with boiling 1% SDS buffer. Resulting protein lysates were quantified and run according to validated immunoblot procedures with the following antibodies: phospho-AKT (Ser473, #4060; Cell Signaling Technology), phospho-AKT (Thr308, #9275; Cell Signaling Technology), AKT (#9272; Cell Signaling Technology), phospho-ERK (Thr202/Thr204, #4370; Cell Signaling Technology), ERK (#9102; Cell Signaling Technology), phospho-S6 (Ser235/236, #2211; Cell Signaling Technology), S6 (#2317; Cell Signaling Technology), NF1 (#A300-140A; Bethyl Laboratories), p120 (#G12920; Trans Labs), RAS (#05-516; Upstate), KRAS (#sc-30; Santa Cruz Biotechnology), HRAS (#sc-520; Santa Cruz Biotechnology), NRAS (#sc-519; Santa Cruz Biotechnology), and MITF (#M3621; Dako). Immunoblots were quantified with ImageJ software.

### *Experimental Animals*

Animal procedures were approved by the Center for Animal and Comparative Medicine in Harvard Medical School (Boston, MA) in accordance with the NIH Guild for the Care and Use of Laboratory Animals and the Animal Welfare Act. A breeding scheme was set up in which mice carrying a conditional *Nf1* allele (*Nf1*<sup>flox/flox</sup> mice; ref. 30) were crossed to mice with a conditional activating mutation in *Braf* (*Braf*<sup>CA/+</sup> mice; ref. 31) and a transgenic mouse strain harboring a tamoxifen-inducible Cre recombinase-estrogen receptor fusion transgene that is under the control of the melanocyte-specific tyrosinase promoter, designated *Tyr::CreERT2* (32). Genotyping was conducted by PCR, as described for every model (30–32). To activate *Tyr::CreERT2*, mice were treated topically with freshly prepared tamoxifen (T5648; Sigma) 2 to 3 months after birth. Tamoxifen (20 mg/mL in 100% ethanol) was applied to a small section of skin on the shaved backs, and the treatment schedule consisted of 4 treatments over 7 days. For all genotypes, pigmentation levels were quantified weekly on a scale from 0 (no pigmentation) to 8 (high pigmentation). To study the contribution of the PI3K/AKT pathway to the observed hyperpigmentation phenotype in the *Tyr::CreERT2*; *Braf*<sup>CA/+</sup>; *Nf1*<sup>flox/flox</sup> mice, animals were treated daily with the PI3K inhibitor GDC-0941 (150 mg/kg, oral gavage) for 8 weeks after *Tyr::CreERT2* induction.

### *Xenograft Studies and Treatments*

For cancer cell xenograft experiments, nude mice were inoculated subcutaneously with  $3 \times 10^6$  human or mouse melanoma cells. Tumor volumes were calculated by measuring length and width of the lesions and with the formula [(length)  $\times$  (width)<sup>2</sup>  $\times$  0.52]. Murine *Braf*/*Nf1*-mutant melanoma cells formed rapidly growing tumors. Two weeks after injection, when tumors were growing in log phase, mice were randomly divided into different treatment groups that were administered the PI3K inhibitor GDC-0941 (150 mg/kg, oral gavage), the mTOR inhibitor rapamycin [5 mg/kg, intraperitoneal (i.p.) injection], the MEK inhibitor PD0325901 (10 mg/kg, oral gavage), the BRAF inhibitor PLX4720 (2.5 mg/kg, i.p.), or the combination of both PD0325901 or PLX4720 and rapamycin. Mice were treated daily for 7 days.

### *Histology, Immunohistochemistry, and SA-β-gal Staining*

Tissues were fixed in formalin, embedded in paraffin, and stained with hematoxylin and eosin (H&E) when indicated. Standard immunohistochemistry and immunofluorescence protocols were followed for S100 (Z0311, 1:400; Dako) staining. An alkaline phosphatase staining method was used for NF1 (ab30325, 1:300; Abcam) immunohistochemistry. Antigen unmasking was conducted by pressure

## RESEARCH ARTICLE

Maertens et al.

cooking in citrate buffer (pH 6). A human melanoma tissue microarray (ME804a; US Biomax Inc.) was used for evaluation of *NF1* expression in malignant and metastatic melanomas. SA- $\beta$ -gal staining was conducted on fresh mouse tissue. Small pieces were fixed for 30 minutes in 3% paraformaldehyde, incubated in SA- $\beta$ -gal staining solution as described (50), and then embedded and sectioned.

***NF1 Mutational Analysis and Data Mining***

The entire *NF1* coding region of 11 human melanoma cell lines (Fig. 5A) was amplified in 5 overlapping reverse-transcription PCR (RT-PCR) fragments and used as the template for direct sequencing, essentially as described (51). Copy number analysis by multiplex ligation-dependent probe amplification (MLPA) was conducted as described (52). The nomenclature of the mutations is based on *NF1* mRNA sequence NM\_001042492.2, with 1 being the first nucleotide of the ATG start codon. Next, publicly available resources providing information on somatic mutations implicated in human melanoma cell lines (53, 54) and primary tumors (55–57) were mined.

**Patient Samples**

Patients with metastatic melanoma containing the *BRAF<sup>V600E</sup>* mutation (confirmed by genotyping) were enrolled in clinical trials for treatment with a *BRAF* inhibitor (vemurafenib) or combined *BRAF*/MEK inhibitors (dabrafenib + trametinib), and their consent was obtained for tissue acquisition per Institutional Review Board (IRB)-approved protocol. Tumor biopsies were conducted pretreatment (day 0), at 10 to 14 days on treatment, and/or at time of progression if applicable. Formalin-fixed tissue was analyzed to confirm that viable tumor was present via H&E staining. Additional tissue was snap frozen and stored in liquid nitrogen.

**Disclosure of Potential Conflicts of Interest**

M. McMahon has commercial research grants from Novartis and Plexxikon. R. Marais is Secretary General of the European Association for Cancer Research, has received honoraria from service on the speakers' bureau for Roche, and is a consultant/advisory board member for Novartis and Servier Research Institute. No potential conflicts of interest were disclosed by the other authors.

**Authors' Contributions**

**Conception and design:** O. Maertens, B. Johnson, K. Cichowski

**Development of methodology:** O. Maertens, B. Johnson, P. Hollstein, R. Marais

**Acquisition of data (provided animals, acquired and managed patients, provided facilities, etc.):** O. Maertens, B. Johnson, P. Hollstein, D.T. Frederick, Z.A. Cooper, L. Messiaen, M. McMahon, K. Flaherty, J.A. Wargo, R. Marais, K. Cichowski

**Analysis and interpretation of data (e.g., statistical analysis, biostatistics, computational analysis):** O. Maertens, B. Johnson, P. Hollstein, L. Messiaen, R.T. Bronson, M. McMahon, K. Flaherty, J.A. Wargo, K. Cichowski

**Writing, review, and/or revision of the manuscript:** O. Maertens, D.T. Frederick, Z.A. Cooper, M. McMahon, K. Flaherty, J.A. Wargo, K. Cichowski

**Administrative, technical, or material support (i.e., reporting or organizing data, constructing databases):** O. Maertens

**Study supervision:** K. Cichowski

**Conducted immunohistochemical analysis:** S. Granter

**Acknowledgments**

The authors thank M. McMahon and K. Haigis for providing the *Braf<sup>CA/+</sup>* mice, L. Chin for providing the *Tyr::CreER<sup>T2</sup>* mice, and L. Garraway for cell lines.

**Grant Support**

K. Cichowski and the majority of this work was supported by the National Cancer Institute (R01 CA111754) and the Ludwig Center at Dana-Farber/Harvard Cancer Center. O. Maertens is a postdoctoral fellow of the Research Foundation Flanders (FWO).

Received July 4, 2012; revised November 14, 2012; accepted November 15, 2012; published OnlineFirst November 21, 2012.

**REFERENCES**

- Courtois-Cox S, Jones SL, Cichowski K. Many roads lead to oncogene-induced senescence. *Oncogene* 2008;27:2801–9.
- Kuilman T, Michaloglou C, Mooi WJ, Peepre DS. The essence of senescence. *Genes Dev* 2010;24:2463–79.
- Bartkova J, Rezaei N, Liontos M, Karakaidos P, Kletsas D, Issaeva N, et al. Oncogene-induced senescence is part of the tumorigenesis barrier imposed by DNA damage checkpoints. *Nature* 2006;444:633–7.
- Di Micco R, Fumagalli M, Cicalese A, Piccinini S, Gasparini P, Luisi C, et al. Oncogene-induced senescence is a DNA damage response triggered by DNA hyper-replication. *Nature* 2006;444:638–42.
- Mallette FA, Gaumont-Leclerc MF, Ferbeyre G. The DNA damage signaling pathway is a critical mediator of oncogene-induced senescence. *Genes Dev* 2007;21:43–8.
- Narita M, Nunez S, Heard E, Narita M, Lin AW, Hearn SA, et al. Rb-mediated heterochromatin formation and silencing of E2F target genes during cellular senescence. *Cell* 2003;113:703–16.
- Courtois-Cox S, Genther Williams SM, Reczek EE, Johnson BW, McGillivray LT, Johannessen CM, et al. A negative feedback signaling network underlies oncogene-induced senescence. *Cancer Cell* 2006;10:459–72.
- Wajapeyee N, Serra RW, Zhu X, Mahalingam M, Green MR. Oncogenic *BRAF* induces senescence and apoptosis through pathways mediated by the secreted protein IGFBP7. *Cell* 2008;132:363–74.
- Acosta JC, O'Loughlin A, Banito A, Guijarro MV, Augert A, Raguz S, et al. Chemokine signaling via the CXCR2 receptor reinforces senescence. *Cell* 2008;133:1006–18.
- Kuilman T, Michaloglou C, Vredeveld LC, Douma S, van Doorn R, Desmet CJ, et al. Oncogene-induced senescence relayed by an interleukin-dependent inflammatory network. *Cell* 2008;133:1019–31.
- Gray-Schopfer VC, Cheong SC, Chong H, Chow J, Moss T, Abdel-Malek ZA, et al. Cellular senescence in naevi and immortalisation in melanoma: a role for p16? *Br J Cancer* 2006;95:496–505.
- Michaloglou C, Vredeveld LC, Soengas MS, Denoyelle C, Kuilman T, van der Horst CM, et al. BRAF<sup>E600</sup>-associated senescence-like cell cycle arrest of human naevi. *Nature* 2005;436:720–4.
- Garnett MJ, Marais R. Guilty as charged: B-RAF is a human oncogene. *Cancer Cell* 2004;6:313–9.
- Dankort D, Curley DP, Cartlidge RA, Nelson B, Karnezis AN, Damsky WE, et al. Braf(V600E) cooperates with Pten loss to induce metastatic melanoma. *Nat Genet* 2009;41:544–52.
- Dhomem N, Reis-Filho JS, da Rocha Dias S, Hayward R, Savage K, Delmas V, et al. Oncogenic Braf induces melanocyte senescence and melanoma in mice. *Cancer Cell* 2009;15:294–303.
- Pollock PM, Harper UL, Hansen KS, Yudt LM, Stark M, Robbins CM, et al. High frequency of *BRAF* mutations in nevi. *Nat Genet* 2003;33:19–20.
- Vredeveld LC, Possik PA, Smit MA, Meissl K, Michaloglou C, Horlings HM, et al. Abrogation of BRAF<sup>V600E</sup>-induced senescence by PI3K pathway activation contributes to melanomagenesis. *Genes Dev* 2012;26:1055–69.
- Bernards A, Settleman J. GAPs in growth factor signalling. *Growth Factors* 2005;23:143–9.
- Dasgupta B, Yi Y, Chen DY, Weber JD, Gutmann DH. Proteomic analysis reveals hyperactivation of the mammalian target of rapamycin pathway in neurofibromatosis 1-associated human and mouse brain tumors. *Cancer Res* 2005;65:2755–60.

20. Johannessen CM, Reczek EE, James MF, Brems H, Legius E, Cichowski K. The NF1 tumor suppressor critically regulates TSC2 and mTOR. *Proc Natl Acad Sci U S A* 2005;102:8573–8.
21. Cancer Genome Atlas Research Network. Comprehensive genomic characterization defines human glioblastoma genes and core pathways. *Nature* 2008;455:1061–8.
22. Ding L, Getz G, Wheeler DA, Mardis ER, McLellan MD, Cibulskis K, et al. Somatic mutations affect key pathways in lung adenocarcinoma. *Nature* 2008;455:1069–75.
23. McGillicuddy LT, Fromm JA, Hollstein PE, Kubek S, Beroukhim R, De Raedt T, et al. Proteasomal and genetic inactivation of the NF1 tumor suppressor in gliomagenesis. *Cancer Cell* 2009;16:44–54.
24. Parsons DW, Jones S, Zhang X, Lin JC, Leary RJ, Angenendt P, et al. An integrated genomic analysis of human glioblastoma multiforme. *Science* 2008;321:1807–12.
25. Holzel M, Huang S, Koster J, Ora I, Lakeman A, Caron H, et al. NF1 is a tumor suppressor in neuroblastoma that determines retinoic acid response and disease outcome. *Cell* 2010;142:218–29.
26. Bosch E, Cherwinski H, Peterson D, McMahon M. Mutations of critical amino acids affect the biological and biochemical properties of oncogenic A-Raf and Raf-1. *Oncogene* 1997;15:1021–33.
27. Zhu J, Woods D, McMahon M, Bishop JM. Senescence of human fibroblasts induced by oncogenic Raf. *Genes Dev* 1998;12:2997–3007.
28. Woods D, Parry D, Cherwinski H, Bosch E, Lees E, McMahon M. Raf-induced proliferation or cell cycle arrest is determined by the level of Raf activity with arrest mediated by p21Cip1. *Mol Cell Biol* 1997;17:5598–611.
29. De Schepper S, Boucneau J, Lambert J, Messiaen L, Naeyaert JM. Pigment cell-related manifestations in neurofibromatosis type 1: an overview. *Pigment Cell Res* 2005;18:13–24.
30. Zhu Y, Romero MI, Ghosh P, Ye Z, Charnay P, Rushing EJ, et al. Ablation of NF1 function in neurons induces abnormal development of cerebral cortex and reactive gliosis in the brain. *Genes Dev* 2001;15:859–76.
31. Dankort D, Filenova E, Collado M, Serrano M, Jones K, McMahon M. A new mouse model to explore the initiation, progression, and therapy of BRAFV600E-induced lung tumors. *Genes Dev* 2007;21:379–84.
32. Bosenberg M, Muthusamy V, Curley DP, Wang Z, Hobbs C, Nelson B, et al. Characterization of melanocyte-specific inducible Cre recombinase transgenic mice. *Genesis* 2006;44:262–7.
33. Ramjaun AR, Downward J. Ras and phosphoinositide 3-kinase: partners in development and tumorigenesis. *Cell Cycle* 2007;6:2902–5.
34. Johannessen CM, Johnson BW, Williams SM, Chan AW, Reczek EE, Lynch RC, et al. TORC1 is essential for NF1-associated malignancies. *Curr Biol* 2008;18:56–62.
35. Ji Z, Flaherty KT, Tsao H. Targeting the RAS pathway in melanoma. *Trends Mol Med* 2012;18:27–35.
36. Bollag G, Hirth P, Tsai J, Zhang J, Ibrahim PN, Cho H, et al. Clinical efficacy of a RAF inhibitor needs broad target blockade in BRAF-mutant melanoma. *Nature* 2010;467:596–9.
37. De Raedt T, Walton Z, Yecies JL, Li D, Chen Y, Malone CF, et al. Exploiting cancer cell vulnerabilities to develop a combination therapy for ras-driven tumors. *Cancer Cell* 2011;20:400–13.
38. Heidorn SJ, Milagre C, Whittaker S, Nourry A, Niculescu-Duvas I, Dhomen N, et al. Kinase-dead BRAF and oncogenic RAS cooperate to drive tumor progression through CRAF. *Cell* 2010;140:209–21.
39. Lin WM, Baker AC, Beroukhim R, Winckler W, Feng W, Marmion JM, et al. Modeling genomic diversity and tumor dependency in malignant melanoma. *Cancer Res* 2008;68:664–73.
40. Smalley KS, Xiao M, Villanueva J, Nguyen TK, Flaherty KT, Letrero R, et al. CRAF inhibition induces apoptosis in melanoma cells with non-V600E BRAF mutations. *Oncogene* 2009;28:85–94.
41. Guldberg P, thor Straten P, Birck A, Ahrenkiel V, Kirkin AF, Zeuthen J. Disruption of the MMAC1/PTEN gene by deletion or mutation is a frequent event in malignant melanoma. *Cancer Res* 1997;57:3660–3.
42. Johannessen CM, Boehm JS, Kim SY, Thomas SR, Wardwell L, Johnson LA, et al. COT drives resistance to RAF inhibition through MAP kinase pathway reactivation. *Nature* 2010;468:968–72.
43. Nazarian R, Shi H, Wang Q, Kong X, Koya RC, Lee H, et al. Melanomas acquire resistance to B-RAF(V600E) inhibition by RTK or N-RAS upregulation. *Nature* 2010;468:973–7.
44. Poulikakos PI, Persaud Y, Janakiraman M, Kong X, Ng C, Moriceau G, et al. RAF inhibitor resistance is mediated by dimerization of aberrantly spliced BRAF(V600E). *Nature* 2011;480:387–90.
45. Shi H, Moriceau G, Kong X, Lee MK, Lee H, Koya RC, et al. Melanoma whole-exome sequencing identifies (V600E)B-RAF amplification-mediated acquired B-RAF inhibitor resistance. *Nat Commun* 2012;3:724.
46. Villanueva J, Vultur A, Lee JT, Somasundaram R, Fukunaga-Kalabis M, Cipolla AK, et al. Acquired resistance to BRAF inhibitors mediated by a RAF kinase switch in melanoma can be overcome by cotargeting MEK and IGF-1R/PI3K. *Cancer Cell* 2010;18:683–95.
47. Paraiso KH, Xiang Y, Rebecca VW, Abel EV, Chen YA, Munko AC, et al. PTEN loss confers BRAF inhibitor resistance to melanoma cells through the suppression of BIM expression. *Cancer Res* 2011;71:2750–60.
48. Shao Y, Aplin AE. Akt3-mediated resistance to apoptosis in B-RAF-targeted melanoma cells. *Cancer Res* 2010;70:6670–81.
49. Cichowski K, Santiago S, Jardim M, Johnson BW, Jacks T. Dynamic regulation of the Ras pathway via proteolysis of the NF1 tumor suppressor. *Genes Dev* 2003;17:449–54.
50. Dimri GP, Lee X, Basile G, Acosta M, Scott G, Roskelley C, et al. A biomarker that identifies senescent human cells in culture and in aging skin *in vivo*. *Proc Natl Acad Sci U S A* 1995;92:9363–7.
51. Messiaen LM, Callens T, Mortier G, Beysen D, Vandebroucke I, Van Roy N, et al. Exhaustive mutation analysis of the NF1 gene allows identification of 95% of mutations and reveals a high frequency of unusual splicing defects. *Hum Mutat* 2000;15:541–55.
52. Wimmer K, Yao S, Claes K, Kehler-Sawatzki H, Tinschert S, De Raedt T, et al. Spectrum of single- and multixon NF1 copy number changes in a cohort of 1,100 unselected NF1 patients. *Genes Chromosomes Cancer* 2006;45:265–76.
53. Barretina J, Caponigro G, Stransky N, Venkatesan K, Margolin AA, Kim S, et al. The Cancer Cell Line Encyclopedia enables predictive modelling of anticancer drug sensitivity. *Nature* 2012;483:603–7.
54. Forbes SA, Bindal N, Bamford S, Cole C, Kok CY, Beare D, et al. COSMIC: mining complete cancer genomes in the Catalogue of Somatic Mutations in Cancer. *Nucleic Acids Res* 2011;39:D945–50.
55. Berger MF, Hodis E, Heffernan TP, Deribe YL, Lawrence MS, Protopopov A, et al. Melanoma genome sequencing reveals frequent PREX2 mutations. *Nature* 2012;485:502–6.
56. Hodis E, Watson IR, Kryukov GV, Arold ST, Imielinski M, Theurillat JP, et al. A landscape of driver mutations in melanoma. *Cell* 2012;150:251–63.
57. Krauthammer M, Kong Y, Ha BH, Evans P, Bacchiocchi A, McCusker JP, et al. Exome sequencing identifies recurrent somatic RAC1 mutations in melanoma. *Nat Genet* 2012;44:1006–14.